J. Plant Biol. (2017) 60:582-592
DOI 10.1007/s12374-017-0224-7

ORIGINAL ARTICLE

# Genetic Analysis of the Tomato *inquieta* Mutant Links the ARP2/3 Complex to Trichome Development

**Na-Rae Jeong[1], Heejin Kim[1], In-Taek Hwang[1,2], Gregg A. Howe[3,4,5] and Jin-Ho Kang[1,2,*]**

[1]*Graduate School of International Agricultural Technology and Crop Biotechnology Institute, Seoul National University, Pyeongchang 25354, Korea*
[2]*Institute of GreenBio Science and Technology, Seoul National University, Pyeongchang 25354, Korea*
[3]*Department of Energy-Plant Research Laboratory, Michigan State University, East Lansing, MI 48824, USA*
[4]*Department of Biochemistry and Molecular Biology, Michigan State University, East Lansing, MI 48824, USA*
[5]*Plant Resilience Institute, Biology, Michigan State University, East Lansing, MI 48824, USA*

Received: June 14, 2017 / Accepted: August 22, 2017


**Abstract** Trichomes are hair-like structures on the aerial surface of many plant species. Trichomes are well characterized for their role as physical barriers and chemical defense against herbivore attack. Here, we describe the characterization of a monogenic recessive mutant of tomato (*Solanum lycopersicum*) called *inquieta* (*ini*). All trichome types on *ini* plants showed distinct morphological defects (e.g., swelling) that are known to be associated with defects in the actin cytoskeleton. Genetic mapping experiments positioned the *Ini* locus within a 1.5 cM interval on chromosome 11 that contains the tomato homolog of the Arabidopsis *ARPC2A* gene, which encodes a protein involved in nucleating the polymerization of actin filaments. Use of *ARPC2A* as a molecular marker showed that this gene strictly co-segregates with the target locus in a mapping population of 135 $F_2$ plants. Reverse transcriptase (RT)-PCR and genomic PCR experiments showed that full-length *ARPC2A* is amplified in wild-type but not in the *ini* mutant. Flanking PCR and Southern blot analysis showed that the *ini* mutation corresponds to a complex ~6-kb insertion in the $5^{th}$ intron of *ARPC2A*. These results provide molecular evidence that altered trichome development in the *ini* mutant is caused by a defect in actin cytoskeleton formation.

**Keywords:** ARP2/3-WAVE complex, *ARPC2A*, *Inquieta*, Map-based cloning, Tomato, Trichome

*Corresponding author; Jin-Ho Kang
Tel : +82-33-339-5831
E-mail : kangjinho@snu.ac.kr

## Introduction

Plant trichomes are hair-like outgrowths originated from aerial epidermis of leaf, hypocotyl, stem, and floral organs in many plant species. Trichomes perform diverse biological functions such as protection against biotic stresses, including insect and pathogen attack (Kennedy 2003; Shepherd et al. 2005) and adaption to abiotic stresses such as water loss and UV-B radiation (Ehleringer and Mooney 1978; Karabourniotis et al. 1992). Trichomes can be classified morphologically as being either non-glandular or glandular, and either unicellular or multicellular. As trichomes are readily accessible structures and may not be critical for plant growth, they serve as an excellent model for studying the developmental processes underlying the cell fate determination, including cell cycle control and cell morphogenesis (Qian et al. 2009; Yang and Ye 2013; Chang et al. 2016).

In the model plant Arabidopsis, which has only one type of unicellular, non-glandular trichome, a transcriptional regulatory network of trichome initiation and development has been elucidated through extensive genetic and molecular analyses. This work has shown, for example, that trichome development is controlled by a trimeric transcriptional complex consisting of R2R3 MYB proteins, basic helix-loop-helix (bHLH) proteins, and a WD40 repeat (WDR) protein. This MYB-bHLH-WDR complex positively regulates the expression of the homeodomain transcription factor GL2 to regulate trichome initiation (Szymanski et al. 1998; Ramsay and Glover 2005; Zhao et al. 2008). Recently, C2H2 zinc finger proteins (ZFPs) including GLABROUS INFLORESCENCE STEMS (GIS) and ZFP5 were identified as upstream transcriptional regulators to control the expression of *MYB* or *bHLH* genes (Gan et al. 2006; Yan et al. 2014). After trichome formation is initiated, tirchome cells are enlarged and develop branches by arresting cell division and switching to the endoreplication programme, which are genetically controlled by several different genes including *SIAMESE* and *ZWICHEL* (Oppenheimer et al. 1997; Walker et al. 2000; Grebe 2012). Finally, the actin-related protein (ARP)2/3 complex involved in nucleating actin filaments, and the WAVE complex that regulates ARP2/3 activity, are required to maintain polarized stalk and branch growth. The 'distorted group' mutants, which are defective in genes encoding components of the ARP2/3 and WAVE complexes, exhibit swollen and twisted trichomes (Basu et al. 2004; Deeks et al. 2004; Szymanski 2005; Uhrig et al. 2007).

Cultivated tomato (*Solanum lycopersicum* L.) and its wild relatives have at least seven distinct types of trichomes that differ with respect to size, cell number, and the presence of glandular secreting cells (Luckwill 1943). Among the non-glandular trichome types (type II, III, and V), type II and type III trichomes are similar in length but differ by the presence of a multicellular and unicellular base, respectively. The shortest type V trichomes have a unicellular base. Among four different glandular trichomes (type I, IV, VI, and VII), type I trichomes have a multicellular base, a long multicellular stalk, and a small glandular tip. Type IV trichomes contain a unicellular base, a short multicellular stalk, and a small secreting glandular tip. Type VI trichomes consist of a four-celled glandular head on a short multicellular stalk, whereas type VII trichomes have a unicellular stalk and an irregularly shaped 4- to 8-celled gland (Luckwill 1943; Kang et al. 2010a). The glandular trichomes have been well characterized as chemical "factories" that produce diverse specialized metabolites implicated in anti-insect defense. For instance, terpenoids, flavonoids, 2-tridecanone and other methyl ketones synthesized in type VI trichomes of cultivated tomato and its wild relatives exert toxic effects on several arthropod pests, including tobacco hornworm (*Manduca sexta*), aphids (*Macrosiphum euphorbiae* and *Myzus persicae*), and Colorado potato beetle (*Leptinotarsa decemlineata*) (Williams et al. 1980; Kennedy 2003; Kang et al. 2010b). Acyl sugars secreted from type IV trichomes of *S. pennellii* play an important role in the resistance to numerous insects such as whiteflies (*Bemisia argentifolii* and *Trialeurodes vaporariorum*), beet armyworm (*Spodoptera exigua*), tomato fruitworms, and aphids (Goffreda et al. 1990; Rodriguez et al. 1993; Juvik et al. 1994; Kennedy 2003). Given the important roles of these compounds in plant protection, recent research has focused on understanding the underlying biochemical pathways required for their synthesis (Sallaud et al. 2009; Schilmiller et al. 2009; Bleeker et al. 2012; Schilmiller et al. 2012; Kang et al. 2014). However, our understanding of how multicellular trichomes develop is still in its infancy and only a few genes controlling trichome development have been identified. For example, the *Woolly* gene encoding a homeodomain-containing transcription factor regulates type I trichome development (Yang et al. 2011). The *Hairless* (*Hl*) gene encoding the SRA1 subunit of the WAVE regulatory complex is required for proper cell enlargement and cell shape of all trichome types in tomato (Kang et al. 2016).

The *inquieta* (*ini*) mutant of tomato was first reported a half-century ago as a radiation-induced mutant that is defective in trichome development (Stubbe 1964). Previous studies have noted that the trichome phenotype of the *ini* and *hl* mutants are similar, with both having severely bent trichomes that impart a granular appearance to aerial tissues (Reeves 1977; Dempsey and Sherif 1987). Subsequent studies showed that *ini* is non-allelic to *hl* and that the *Ini* locus is located on the short arm of chromosome 11 (Zobel et al. 1970; Tanksley et al. 1992). Here, we analyzed the effect of *ini* on trichome morphology and also used a map-based cloning approach to identify candidate genes for *Ini*. Our results show that the *ARPC2A* gene, which encodes a subunit of ARP2/3 complex, strictly cosegregates with *ini* in an $F_2$ mapping population. Molecular analyses revealed a DNA insertion in the *ARPC2A* gene of *ini* mutant plants, and also showed that this insertion is associated with the loss of detectable expression of *ARPC2A* transcripts. These collective data provide compelling evidence that altered trichome development in the *ini* mutant is caused by a defect in *ARPC2A*.

## Results

### Effect of *ini* on Trichome Development

We used light microscopy to compare the morphology of trichomes on leaves, stems, hypocotyls, and floral organs of the *ini* mutant to its wild-type parent (cv Rheinlands Ruhm). Compared to wild-type in which type I trichomes were aligned perpendicular to the epidermal surface, *ini* showed highly twisted and swollen trichomes (Fig. 1). The identity of the distorted structures of *ini* as type I trichomes was confirmed by low temperature scanning electron microscopy (Cryo-SEM). This analysis showed that type I trichomes on the *ini* mutant contain highly swollen cells that fail to orient perpendicular to the epidermal surface, resulting in highly distorted and twisted structures (Fig. 2). Other trichome types on the *ini* mutant also showed swollen and distorted structures. Especially, the type VI trichome, which contains a short neck cell that connects the four-celled glandular head to the stem, showed irregular patterns of cell division on the *ini* mutant. The neck cell of type VI trichomes on the *ini* mutant also protruded from the side of the stem (Fig. 2).

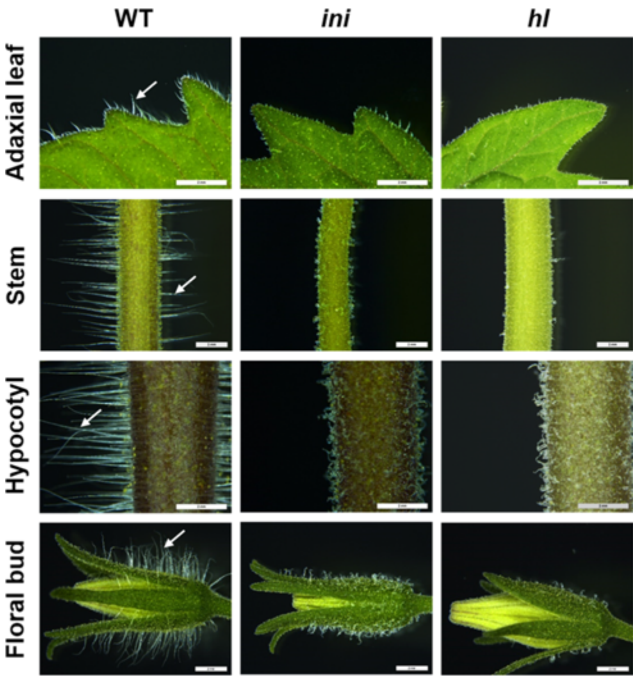


**Fig. 1.** Light micrographs of trichomes on the leaf, stem, hypocotyl, and floral bud of WT, *ini*, and *hl* plants. Photographs show the adaxial leaf surface (first row), stem (second row), hypocotyl (third row), and floral bud (forth row) of each genotype. Arrows indicate representative type I trichomes. All scale bars represent 2 mm.

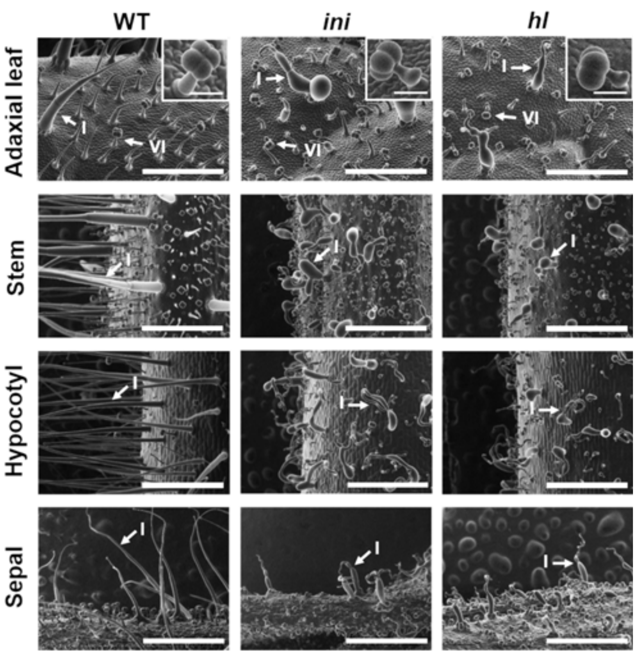


**Fig. 2.** Cryo-SEM micrographs of trichomes on the leaf, stem, hypocotyl, and sepal of WT, *ini*, and *hl* plants. Photographs show the adaxial leaf surface (first row), stem (second row), hypocotyl (third row), and sepal (forth row) of each genotype. Scale bars represent 500 μm in the leaves, 50 μm in the insets, and 1 mm in the stems, hypocotyls, and sepals. Type I and VI trichomes are indicated by arrows.

Previously we reported that aerial tissues of the tomato *hl* mutant have swollen and distorted trichomes (Kang et al. 2010a). Comparison of the *ini* and *hl* mutants showed that their distorted trichome phenotypes are strikingly similar (Fig. 1 and 2), suggesting that the *ini* and *hl* mutations affect similar developmental processes.

Genetic Mapping of *Ini*

$F_1$ plants derived from a cross between *ini* and its wild-type parent showed normal trichome phenotypes, indicating that the mutation is recessive. An $F_2$ population obtained by selfing the $F_1$ plants was scored at the seedling stage (3-week-old plants) for the trichome distortion phenotype. Among 116 $F_2$ plants, 27 plants exhibited trichome distortion, whereas the remaining $F_2$ plants appeared normal. This ratio (3.3:1) is in good agreement with that predicted for a single recessive mutation ($\chi^2$ = 0.18; $P$ = 0.67). Owing to the similar trichome phenotype between the *ini* and *hl* mutants, we generated $F_1$ plants derived from a cross between *ini* and *hl* plants to test for genetic complementation between *ini* and *hl*. All $F_1$ plants obtained from six independent crosses showed normal trichome development, indicating that *Ini* and *Hl* are different genes.

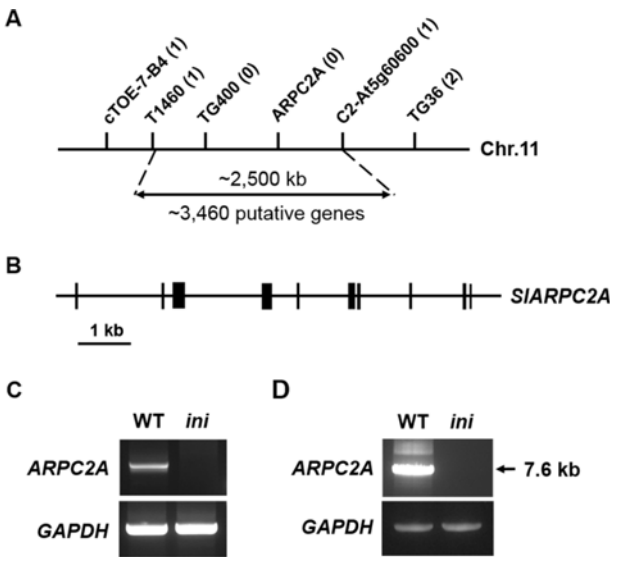


**Fig. 3.** The *ini* mutation cosegregates with the tomato homolog of *ARPC2A*. (A) Genetic mapping of *Ini* delimited the target gene to an interval between marker T1460 and C2-At5g60600 on tomato chromosome 11. Numbers in parentheses indicate the number of recombination events identified between markers and the target gene. (B) Structure of *SlARPC2A*. Vertical black lines depict exons and horizontal lines indicate intervening introns or intergenic regions. (C) RT-PCR for full length *ARPC2A* from WT and *ini* leaves. *Glyceraldehyde 3-phosphate dehydrogenase* (*GAPDH*) mRNA was used as a loading control. (D) PCR for full length *ARPC2A* genomic DNA from WT and *ini* plants. Genomic DNA of *GAPDH* was used as a positive control of DNA amplification.

*Ini* was previously mapped to the short arm of chromosome 11 near the RFLP marker TG36 (Tanksley et al. 1992). Among the introgression lines (ILs) derived from a cross between *S. lycopersicum* cv. M82 (LA3475) and *S. pennellii* (LA0716), the IL11-3 (LA4094) line contains TG36 (Eshed and Zamir 1995). We used a population of 135 $F_2$ plants derived from a cross between *ini* (LA0953) and IL11-3 to refine the map position of *Ini* using additional markers (Table S1) located in the IL11-3 region. The results indicated that markers T1460 and C2_At5g60660 are most closely linked to *Ini*, with one recombination event identified between *Ini* and each of these markers (Fig. 3A). The ~22,000 kb region defined by T1460 and C2_At5g60660 is predicted to contain approximately 790 hypothetical genes (ITAG2.4 gene models; https://solgenomics.net/) (Fig. 3A).

## *Ini* Likely Encodes the Tomato Homolog of ARPC2A

Recently, we demonstrated that *Hl* encodes the tomato homolog of SRA1, which is a subunit of the highly conserved WAVE regulatory complex involved in actin filament nucleation in eukaryotic cells (Kang et al. 2016). Studies with Arabidopsis have shown that mutations affecting the ARP2/3 and WAVE complexes, which control the formation of the actin cytoskeleton, also cause abnormally distorted trichomes (Basu et al. 2004; El-Assal et al. 2004; Szymanski 2005). To test the hypothesis that *Ini* may encode a component of the ARP2/3-WAVE complex, we identified putative tomato homologs of the known subunits of the Arabidopsis ARP2/3 and WAVE complexes (Szymanski 2005) (Table 1). Only one gene (Solyc11g068610) was located in the region between markers T1460 and C2_At5g60600. Solyc11g068610 is predicted to encode the ARPC2A subunit of the ARP2/3 complex. To further test the genetic relationship between Solyc11g068610 and *Ini*, we developed a CAPS marker for *SlARPC2A* (ARPC2A, Table S1) and tested recombination events in the $F_2$ mapping population. The results showed that the ARPC2A marker strictly co-segregated with *Ini* in the population of 135 $F_2$ plants (Fig. 3A), suggesting that *ARPC2A* and *Ini* are the same gene.

*SlARPC2A* consists of 10 exons and 9 introns, and its genomic and coding DNA sequence are 7,582 and 987 bp in length, respectively (Fig. 3B and Fig. S1A). We used a reverse transcription (RT)-PCR assay to test whether *ini* plants are affected in the expression of *SlARPC2A*. The result showed that *ARPC2A* transcripts were expressed in wild-type leaves but not in *ini* leaves (Fig. 3C). Moreover, genomic PCR analysis showed that full-length genomic DNA of *ARPC2A* was amplified in wild-type but not in *ini* plants (Fig. 3D). These results provide compelling molecular evidence that *Ini* corresponds to *ARPC2A,* which is consistent with the established role of this ARP2/3 complex subunit in regulating actin cytoskeleton formation (Deeks et al. 2004; El-Assal et al. 2004).

*SlARPC2A* is predicted to encode for a 328-amino-acid

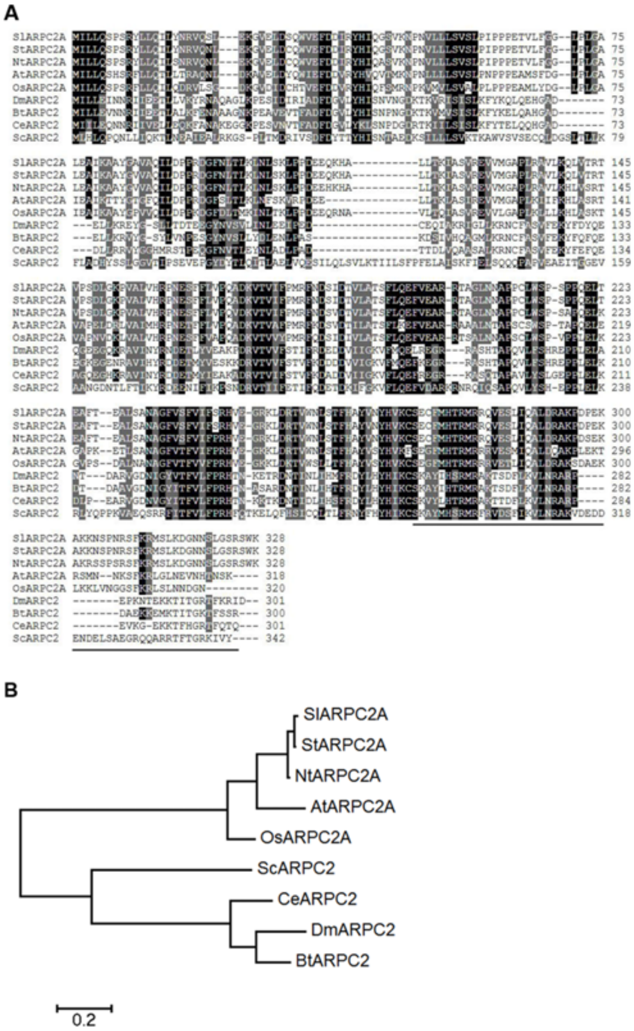


**Fig. 4.** Similarity of ARPC2 between tomato and other species. (A) Comparison of the predicted amino acid sequence of ARPC2A in tomato and other species. Amino acid residues in black indicate identity, and those in gray indicate conserved substitutions. The C-terminal alpha-helix of 43 residues of BTARPC2 that associates with APRC4 (p20) is underlined. *S. lycopersicum* SlARPC2A (Solyc11g068610), *S. tuberosum* StARPC2A (XP_006362875), *N. tabacum* NtARPC2A (NP_001311940), *O. sativa* OsARPC2A (XP_015612421), *A. thaliana* AtARPC2A (NP_564364), *D. melanogaster* DmARPC2 (NP_610033), *B. Taurus* BtARPC2 (1K8K_D), *C. elegans* CeARPC2 (NP_741088) and *S. cerevisiae* ScARPC2 (NP_014433). (B) Phylogenic tree of ARPC2 in tomato and other species. The unrooted phylogenetic tree was constructed by the Maximum Likelihood method using MEGA7 with amino acid sequences of ARPC2 from nine different species. *S. lycopersicum* SlARPC2A (Solyc11g068610), *S. tuberosum* StARPC2A (XP_006362875), *N. tabacum* NtARPC2A (NP_001311940), *A. thaliana* AtARPC2A (NP_564364), *O. sativa* OsARPC2A (XP_015612421), *S. cerevisiae* ScARPC2 (NP_014433), *C. elegans* CeARPC2 (NP_741088), *D. melanogaster* DmARPC2 (NP_610033) and *B. Taurus* BtARPC2 (1K8K_D)

protein having a molecular mass of ~34 kDa (Fig. S1B). Sequence alignment of SlARPC2A with homologs from diverse species indicated that the tomato protein is very similar (>70% identity) to other plant homologs and less similar (21~24%) to ARPC2s from metazoan species (Fig. 4A). Based on the crystal structure of the bovine ARP2/3 complex, the C-terminal domain of vertebrate ARPC2 forms an extended alpha-helix that makes multiple contacts with ARPC4 (Robinson et al. 2001). This C-terminal domain is well conserved among the different species, including tomato. Phylogenetic analysis showed that plant ARPC2As cluster as a distinct phylogenetic clade relative to ARPC2s in yeast and animals (Fig. 4B).

### *ini* Plants Contain a Complex Rearrangement in the *ARPC2A* Gene

The inability to PCR amplify the full-length *ARPC2A* mRNA or genomic DNA from the *ini* mutant, suggested that the structure of this gene is altered in the *ini* mutant. To test this hypothesis, we attempted to amplify four regions (1 – 4) that span the gene (Fig. 5A). Whereas PCR products corresponding to regions 1, 2, and 4 were amplified from genomic DNA isolated from both WT and *ini* plants, region 3 was not amplified from *ini* genomic DNA (Fig. 5B). We employed a similar PCR-based strategy to identify the subregion (i.e., region 7) within region 3 that harbored the putative DNA polymorphism (Fig. 5A, B). Further PCR experiments delimited the polymorphism, as determined by lack of PCR amplification, to a 360 bp fragment (i.e., region 8) within region 7. Repeated attempts to amplify the region 8 from *ini* genomic DNA were unsuccessful, suggesting that intron 5 of *ARPC2A* in the *ini* mutant may harbor a large insertion.

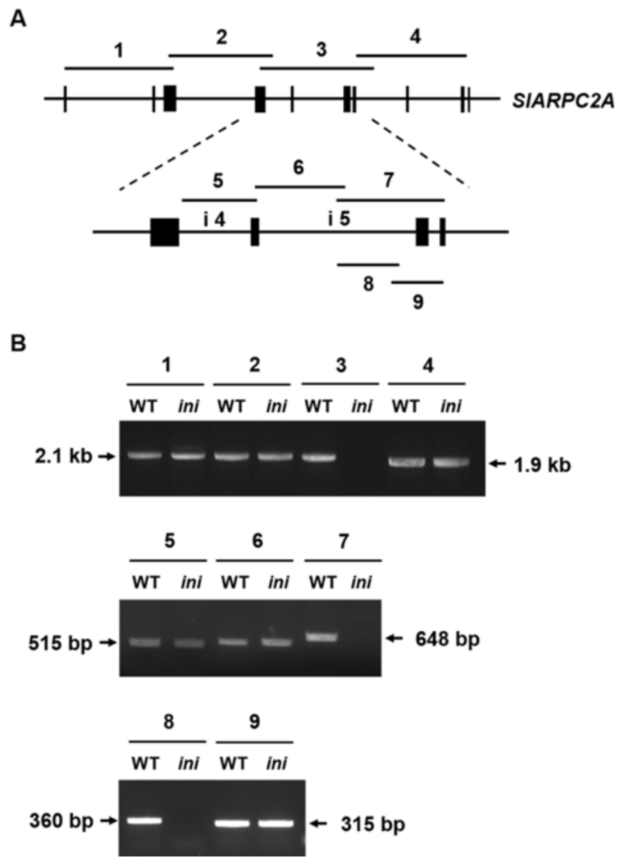


**Fig. 5.** PCR amplification of partial length *ARPC2A* genomic DNA from WT and *ini* plants. (A) Schematic diagram showing PCR-amplified genomic DNA region (1 ~ 9) of *ARPC2A* gene. i 4: intron 4, i 5: intron 5. (B) Agarose gel showing the PCR-amplified products indicated in panel (A).

We used flanking PCR analysis (Thole et al. 2009) to further explore the nature of the polymorphism in intron 5 of the *ini ARPC2A* gene (Fig. 6A). DNA sequencing of PCR fragments that flank intron 5 from *ini* plants revealed that a part of zinc finger protein-related gene (Solyc11g045230) was incorporated into the intron 5 region of *ARPC2A*. The left and right flanking regions contained a ~600 bp DNA fragment (3' intergenic region of Solyc11g045230) and a ~340 bp DNA fragment (part of exon 5, intron 5, exon 6, and 3' UTR region of Solyc11g045230), respectively (Fig. 6B, Fig. S2). DNA sequence alignments showed that these two fragments do not overlap, which implies that an additional DNA fragment is inserted into the mutant form of *ARPC2A*. We used two different DNA probes (probes 1 and 2) in Southern blot experiments to confirm the insertion-deletion (indel) polymorphism in this region (Fig. 7). DNA hybridizations performed with probes 1 and 2 clearly revealed ~4.9 kb and ~1.5 kb size polymorphisms, respectively, in genomic DNA from *ini* plants (Fig. 7B). These data demonstrate that the *ini* mutant harbors a complex indel mutation in intron 5 of *ARPC2A*, resulting in lack of expression of a functional *ARPC2A* transcript.

## Discussion

The availability of numerous trichome-related mutants of Arabidopsis has been instrumental for elucidating the molecular mechanisms underlying the development of simple unicellular trichomes. For example, molecular genetic studies with the 'distorted group' (*dis*) of trichome mutants showed that actin filament organization is crucial for cell growth and cell shape in the late stage of trichome development (Basu et al. 2004; Basu et al. 2005; Le et al. 2006; Uhrig et al. 2007). The Arabidopsis *dis* genes encode subunits of two different complexes: the ARP2/3 complex that controls nucleation of actin filaments and the WAVE complex that regulates the activity of ARP2/3. The ARP2/3 complex consists of seven subunits (ARP2, ARP3, ARPC1, ARPC2, ARPC3, ARPC4,

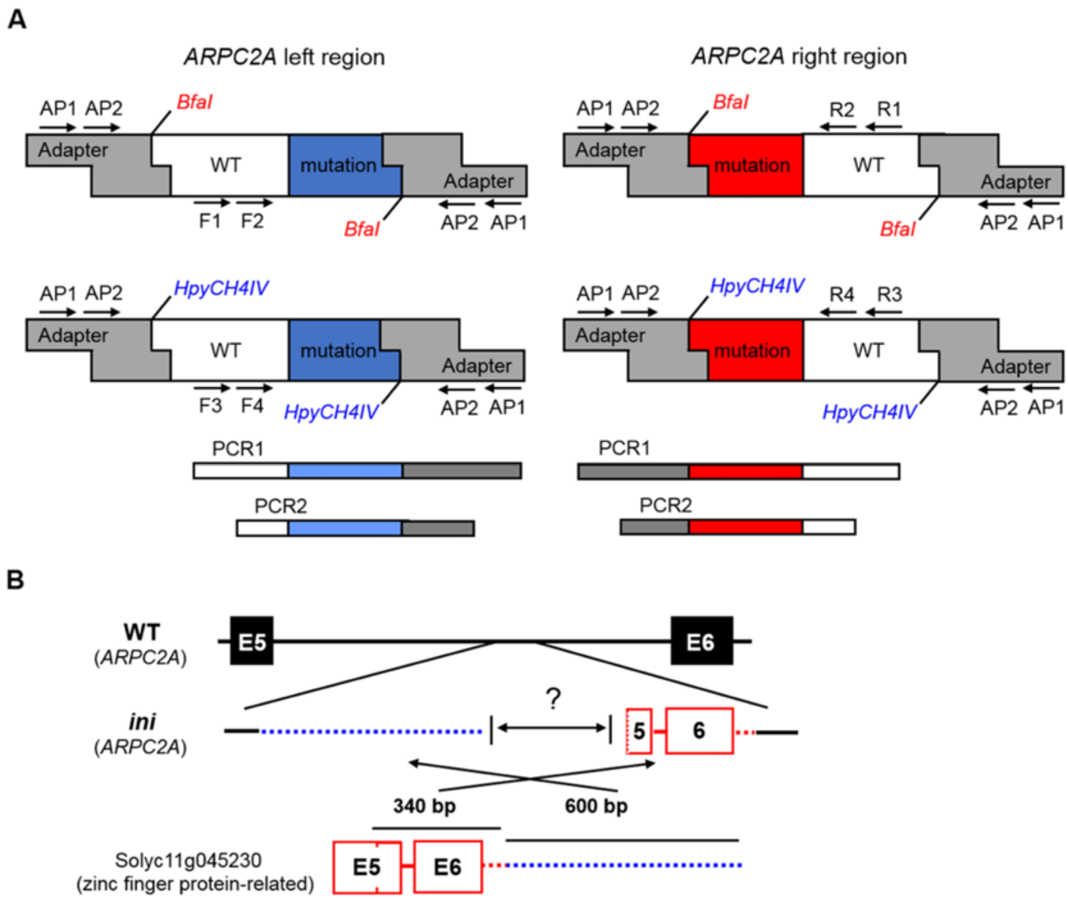


**Fig. 6.** Flanking PCR to analyze mutated sequence within *ARPC2A* gene of *ini* mutant. (A) Diagram depicting flanking regions adjacent to the left or right region of *ARPC2A* DNA in *ini* mutant. A detailed flanking PCR procedure is described in the flanking PCR section of Materials and Methods. Briefly, *Bfa*I- or *HpyCH4*IV-digested DNA was ligated with *Bfa*I or *HpyCH4*IV adapter. The first PCR was carried out with AP1 primer and one of F1, R1, F3, and R3 primers to amplify PCR1 product. Using PCR1 product as a template, the second PCR was carried out with AP2 primer and one of F2, R2, F4, and R4 primers to generate PCR2 product. PCR2 DNA fragment was sequenced to identify mutated sequence within *ARPC2A* gene of *ini* mutant. (B) Diagram depicting the nature of the DNA fragment insertion in *ARPC2A* of *ini* mutant, as compared to *ARPC2A* of WT. The *ini* mutation corresponds to a ≥940-bp insertion (Solyc11g045230: zinc finger protein-related gene) in the intron 5 region of the gene. One-way arrows depict the directionality of zinc finger protein-related gene DNA segments that are inserted in *ARPC2A* of the mutant. A two-way arrow indicates the length of insertion that are not characterized. E5: Exon 5, E6: Exon 6.

and ARPC5), whereas the WAVE complex contains five subunits (NAP1, SRA1, BRICK1, SCAR2, and ABI1L1) (Table 1) (Szymanski 2005). Recently, we reported that the tomato *hl* mutant has abnormally distorted and swollen trichomes very similar to trichomes of Arabidopsis *dis* mutants, and that *Hl* gene encodes the tomato homolog of SRA1, a subunit of WAVE complex (Kang et al. 2016). Here, we provide further genetic evidence that a subunit of ARP2/3 complex is essential for normal trichome development in tomato.

Our map-based cloning study positioned *Ini* in a region spanning markers T1460 and C2_At5g60660 on chromosome 11. Based on the similar trichome phenotype of the *hl* mutant and the *dis* mutants of Arabidopsis, we hypothesized that *Ini* may encode a component of the ARP2/3 or WAVE complex. This approach identified the tomato ortholog of *ARPC2A* as a strong candidate gene for *Ini*. Our results demonstrate that the *ini* mutant harbors a major polymorphism in *ARPC2A* and that this indel is associated with lack of detectable expression of normal *ARPC2A* transcripts in the mutant. However, complementation of *ini* plants with WT *ARPC2A* will be needed to prove that *ARPC2A* is the causal mutation of *ini*. The crystal structure of bovine ARP2/3 complex revealed that the C-terminal domain of ARPC2 interacts with ARPC4 (Robinson et al. 2001). El-Assal et al. demonstrated that ARPC2 physically interacts with ARPC4 in Arabidopsis (2004). We speculate that disrupted interaction between ARPC2A and ARPC4 in the *ini* mutant may impair actin filament nucleation to give rise the aberrant trichome morphology. Validation of this hypothesis will require additional studies, including functional complementation of the *ini* mutant with the normal *ARPC2A* gene.

In addition to tomato and Arabidopsis, several studies

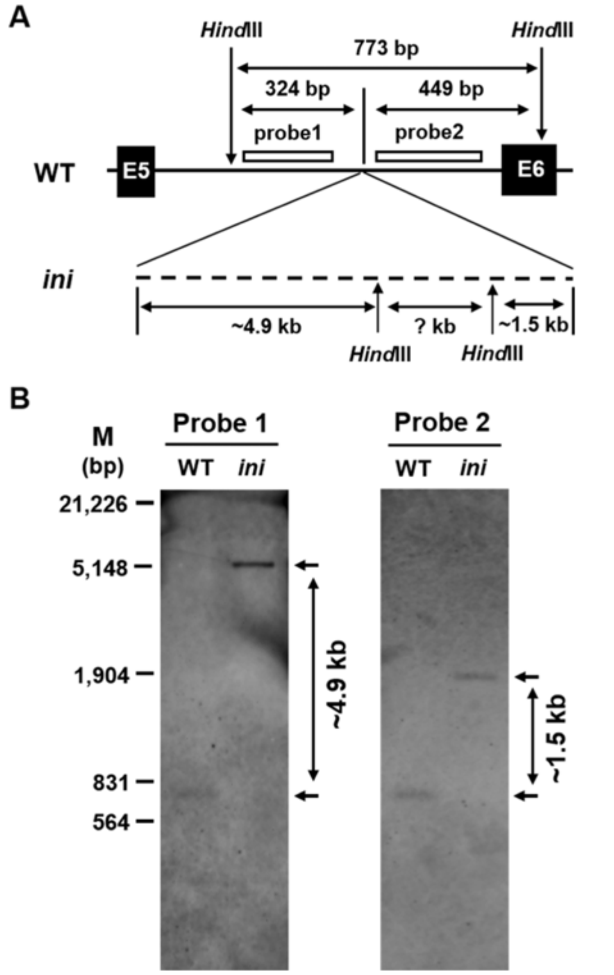


**Fig. 7.** Southern blot analysis with *ARPC2A* probes on genomic DNA extracted from WT and *ini* plants. (A) Schematic diagram showing relative positions of exons, probes, and *Hind*III restriction enzyme sites in *ARPC2A*. *ARPC2A* of *ini* mutant has a DNA insertion (≥ 6.4 kb) between probe 1 and probe 2 in the intron 5 region. E5: Exon 5, E6: Exon 6. (B) Southern blot hybridization of *Hind*III-digested DNA with probe1 and probe2 from WT and *ini* plants. DNA maker (M) sizes (bp) are shown in the left. One-way arrows indicate detected bands. Two-way arrows depict the size difference between bands detected in WT and *ini* plants.

have demonstrated that genes encoding subunits of the ARP2/3 and WAVE complexes in other plants are also important for epidermal cell morphogenesis. For example, the rice mutants *less pronounced lobe epidermal cell* (*lpl*)*2* and *lpl3* that encode SRA1 and NAP1, respectively, show an epidermal cell defect (Zhou et al. 2016). The *arpc1* mutant in *Lotus japonicas* and the *required for infection thread* (*rit*) mutant encoding NAP1 in *Medicago truncatula* also show a trichome distortion phenotype (Miyahara et al. 2010; Hossain et al. 2012). A soybean *gnarled* trichome mutant is impaired in *NAP1* gene (Campbell et al. 2016). These collective observations imply that the function of ARP2/3-WAVE complex in epidermal cell development is evolutionarily conserved in higher plant species. In contrast, trichome initiation in Arabidopsis and tomato may be regulated by distinct transcriptional networks (Serna and Martin 2006). For example, overexpression of Arabidopsis *GL1*-encoding MYB protein in tobacco does not induce trichome formation (Payne et al. 1999). Likewise, overexpression in Arabidopsis of the tomato *Woolly* gene, which encodes a HD-ZIP protein, also does not alter trichome initiation (Yang et al. 2011). Identification of additional tomato mutants that are defective in trichome initiation promises to provide a better understanding of genetic regulatory networks underlying multicellular trichome development.

Several previous studies indicate that the function of ARP2/3 and WAVE complexes is not limited to trichome development. For example, Arabidopsis ARP2, ARP3, and ARPC2 play an important role in stomatal movement by reorganizing actin filaments and vacuoles in guard cells (Jiang et al. 2012; Li et al. 2013). Arabidopsis ARP2 regulates mitochondrial-dependent calcium signaling in response to salt stress (Zhao et al. 2013). Arabidopsis NAP1 acts as a regulator of autophagy in response to nitrogen starvation and salt stress (Wang et al. 2016). The Arabidopsis ARP2/3 and WAVE complexes also modulate light-induced root elongation by controlling the expression of longitudinal F-actin through photoreceptors and the 26S proteasome (Dyachok et al. 2011). In rice, the *early senescence1* mutant encoding SCAR-LIKE PROTEIN2 exhibits higher stomatal density, resulting in excessive water loss (Rao et al. 2015). The tomato *Hl* gene encoding SRA1 is involved in the production of terpenoids and flavonoids (Kang et al. 2016). In addition, ARP2/3-WAVE complex is also required for rhizobial infection of root hair in leguminous plants such as *Lotus japonicas* and *Medicago truncatula* (Miyahara et al. 2010; Hossain et al. 2012; Gavrin et al. 2015; Qiu et al. 2015). The tomato *ini* mutant described here should provide a useful tool to further unravel the diverse functions of the actin cytoskeleton in plants.

## Materials and Methods

### Plant Materials and Growth Conditions

Tomato (*Solanum lycopersicum*) cv Rheinlands Ruhm (accession number LA0535) was used as the wild-type (WT) for all experiments. Seeds for WT and *inquieta* (*ini*, accession number LA0953) were obtained from C.M. Rick Tomato Genetics Resource Center (University of California, Davis). Seedlings were grown in Jiffy peat pots (Hummert International, Earth City, MO, USA) in a growth chamber maintained under 16 h of light (150 μmol $m^{-2}$ $s^{-1}$) at 24°C and 8 h of dark at 18°C and 60% humidity. Three- to four-week-old plants were sampled for trichome morphological analysis.

### Analysis of Trichome Morphology

A dissecting microscope (Leica M205A, Wetzlar, Germany) equipped with LED5000 RL light sources (Leica, Wetzlar, Germany) and a

**Table 1.** Arabidopsis genes encoding subunits of the ARP2/3 and WAVE complexes and their homologs in tomato

| Arabidopsis | | | Tomato* | | |
|---|---|---|---|---|---|
| Genetic name | Gene name | Locus code | Locus code* | E value[†] | Identity with Arabidopsis Homolog (%)[†] |
| *WURM* | *ARP2* | AT3G27000 | Solyc02g094320 | 0 | 90 |
| *DIS1* | *ARP3* | AT1G13180 | Solyc05g013940 | 0 | 83 |
| | | | Solyc04g024530 | 0 | 82 |
| | *ARPC1A* | AT2G30910 | Solyc05g006470 | 0 | 76 |
| | *ARPC1B* | AT2G31300 | Solyc05g006470 | 0 | 76 |
| *DIS2* | *ARPC2A* | AT1G30825 | **Solyc11g068610** | 1.00E-162 | 69 |
| | *ARPC2B* | AT2G33385 | Solyc09g090550 | 1.00E-136 | 52 |
| | *ARPC3* | AT1G60430 | Solyc07g007630 | 1.00E-111 | 86 |
| | | | Solyc02g014540 | 1.00E-60 | 73 |
| | *ARPC4* | AT4G14147 | Solyc12g098430 | 1.00E-113 | 92 |
| *CRK* | *ARPC5A* | AT4G01710 | Solyc01g090450 | 3.00E-82 | 86 |
| *GRL* | *NAP1* | AT2G35110 | Solyc02g068720 | 0 | 76 |
| *PIR/KLK* | *SRA1* | AT5G18410 | **Solyc11g013280** | 0 | 78 |
| | | | **Solyc11g013290** | 0 | 90 |
| *BRK1* | *BRICK1* | AT2G22640 | Solyc03g043720 | 2.00E-50 | 90 |
| *DIS3* | *SCAR2* | AT2G38440 | Solyc09g014980 | 1.00E-115 | 49 |
| | | | Solyc02g076840 | 5.00E-59 | 51 |
| | *ABI1L1* | AT2G46225 | Solyc01g095280 | 1.00E-114 | 60 |

*: Tomato homologs of Arabidopsis ARP2/3 and WAVE complex genes were identified by a blast search using Tomato genome chromosomes (build SL2.5) in the Sol Genomics Network (https://solgenomics.net/). †: E value and identity were obtained by aligning each homolog in tomato and Arabidopsis using blastp in the National Center for Biotechnology Information (https://www.ncbi.nlm.nih.gov/).

Leica MC170 HD Camera (Leica, Wetzlar, Germany) was used to view trichome morphology. The images were analyzed with Leica Application Software (LAS v4.8) and assembled with Photoshop Imaging Suite. To examine trichome morphology in detail, Cryo Scanning Electron Microscopy (CryoSEM) was performed using a Tabletop Microscope TM3030plus (Hitachi High-Technologies Corporation, Tokyo, Japan) equipped with DEBEN coolstage (Deben, London, UK) for freezing and fixing tissues. The images were captured using 15kV to minimize surface charging of the trichomes. The images were analyzed with TM3030plus application software (ver. 01-05-02) and assembled with Photoshop Imaging Suite. All measurements were performed on WT and *ini* plants grown side-by-side in the same growth chamber.

Genetic Mapping of *Ini*

Fine mapping of *Ini* was performed with an $F_2$ population derived from a cross between *ini* mutant (LA0953) and *S. pennellii* introgression line IL11-3 (LA4094), and was facilitated by the tomato genome sequence (Tomato Genome Consortium 2012). A population of 135 $F_2$ plants was scored for the distorted trichome phenotype and subsequently genotyped with PCR-based conserved ortholog markers located within the introgressed region of chromosome 11 (Tomato-EXPEN 2000 map; https://solgenomics.net). Two plants showing recombination between markers T1460 and C2_At5g60600 were identified. Primer sequences used for mapping are listed in Table S1. The TG400 and ARPC2A markers co-segregated with the *Ini* target locus. Genomic DNA extraction and PCR conditions were as described previously (Kang et al. 2010b)

RT-PCR and Genomic DNA PCR

RNA extracted from leaves (TRIzol Reagent, Thermo Fisher Scientific) was used for cDNA synthesis (Thermoscript RT-PCR system, Invitrogen) according to the manufacturer's instructions. Full-length cDNAs corresponding to *SlARPC2A* were amplified by PCR (GeneAmp PCR System 9700, Applied Biosystems), using the ARPC2A-full primer set (Table S2). A cDNA encoding glyceraldehyde 3-phosphate dehydrogenase (GAPDH) was PCR-amplified using the GAPDH primer set (Table S2) and used as a loading control. Reverse transcription (RT)-PCR reactions (50 μL) contained 2 μL cDNA, 1 μL 10 μM solution of each primer, 4 μL dNTP mixture (2.5 mM each), 5 μL 10X Ex Taq buffer, and 0.25 μL TaKaRa Ex Taq polymerase (TaKaRa). The amplification protocol included an initial 30 s denaturation step at 98°C, followed by 30 cycles in which the template was denatured for 10 s at 98°C, annealed for 30 s at 55°C, and extended for 90 s at 72°C. Amplified DNA products were separated on a 1% agarose gel. Full-length and partial genomic DNA fragments corresponding to *SlARPC2A* from WT and *ini* plants were PCR-amplified using the following primer sets (full-length: ARPC2A-full, partial length: ARPC2A-gDNA1 ~ ARPC2A-gDNA9) listed in Table S2. PCR reactions (50 μL) contained 2 μL gDNA template, 1 μL of a 10 μM solution of each primer, 4 μL dNTP mixture (2.5 mM each), 5 μL of 10X Ex-Taq buffer, and 0.25 ul of TaKaRa Ex Taq polymerase (TaKaRa). Amplicons were produced by an initial 2 min denaturation step at 98°C, followed by 30 cycles in which the template was denatured for 10 s at 98°C, annealed for 30 s at 53°C or 55°C, and extended for 2~10 min at 72°C, followed by a final incubation for 5 min or 10 min at 72°C. Amplified products were separated on a 1% agarose gel. Automated nucleotide sequencing was performed at Cosmogenetech (Seoul, Korea).

Amino Acid Alignment and Phylogenetic Analysis

ARPC2 amino acid sequences from *S. lycopersicum* SLARPC2A (Solyc11g068610), *S. tuberosum* STARPC2A (XP_006362875), *N.*

*tabacum* NTARPC2A (NP_001311940), *O. sativa* OSARPC2A (XP_015612421), *A. thaliana* ATARPC2A (NP_564364), *D. melanogaster* DMARPC2 (NP_610033), *B. Taurus* BTARPC2 (1K8K_D), *C. elegans* CEARPC2 (NP_741088) and *S. cerevisiae* SCARPC2 (NP_014433) were aligned using CLUSTALW. In CLUSTALW, the gap-opening and gap-extension penalties were set at 10 and 0.1, respectively, and the alignment was refined by using color align conservation (http://www.bioinformatics. org/sms2/index. html). The phylogenetic tree was constructed with the Maximum Likelihood method based on the JTT matrix-based model in MEGA7.

Flanking PCR

To characterize sequence changes within *ARPC2A* gene of *ini* plants, flanking PCR was performed as described previously with slight modification (Thole et al. 2009). Briefly, genomic DNA of WT and *ini* plants was digested with *Bfa*I or *HpyCH4*VI. For *Bfa*I adapter preparation, ADP2 and ADP3 primers (Table S3), and for *HpyCH4*VI adapter preparation, ADP2 and ADP4 primers (Table S3) were used. After ligation between the *Bfa*I-digested genomic DNA and the *Bfa*I adapter, the first PCR reaction was carried out using the forward primer *ini* fAP1-F1 or the reverse primer *ini* fAP1-R1 in the intron 5 region of *ARPC2A* and the AP1 universal primer in the adapter (Table S3). After the first PCR amplification, a second PCR amplification was performed with the primer closer to the mutation region (*ini* fAP1-F2 or *ini* fAP1-R2) and the AP2 universal primer in the adapter (Table S3). For *HpyCH4*VI-digested genomic DNA ligated with *HpyCH4*VI adapter, the first PCR reaction was carried out using the forward primer *ini* fAP1-F3 or the reverse primer *ini* fAP1-R3 in the intron 5 region of *ARPC2A* gene and the AP1 universal primer in the adapter (Table S3). The second PCR amplification was performed with *ini* fAP1-F4 or *ini* fAP1-R4 primer, and the AP2 universal primer in the adapter (Table S3). Flanking PCR condition included an initial 3 min denaturation step at 95°C, followed by 30 cycles in which the template was denatured for 20 sec at 95°C, annealed for 40 sec at 58°C, and extended for 2 min at 72°C, followed by a final incubation for 5 min at 72°C. Amplified PCR products were gel-purified using a Gel and PCR clean up kit (Cosmogenetech, Seoul, Korea) and sequenced to identify the inserted sequence in *ARPC2A* of *ini* mutant.

Genomic DNA Southern Blot Analysis

Ten μg genomic DNA from WT and *ini* plants was digested with *Hind*III, electrophoresed on a 1% agarose gel, and blotted onto nylon membrane (Amersham Hybond-N+, GE Healthcare Life Science, Chicago, USA). To prepare template DNA for probes of *ARPC2A*, genomic DNA of WT plants was amplified with ARPC2A-gDNA6-F and ARPC2A-gDNA3-R primers (Table S4) spanning exon 5 to intron 7 region. The amplified PCR products were gel-purified using a Gel and PCR clean up kit (Cosmogenetech, Seoul, Korea). Five ng of the gel-purified template DNA was re-amplified with ini-probeT-F1 and ARPC2ACG-R1 primers (Table S4) for probe1 (229 bp), or ini-probeB-F1 and ini-probeB-R1 primers (Table S4) for probe2 (322 bp), using PCR DIG Probe synthesis Kit (Roche Applied Science, Mannheim, Germany). The reamplified PCR products were gel-purified using a Gel and PCR clean up kit (Cosmogenetech, Seoul, Korea). All other steps of Southern blot procedure were performed as described previously (Lee et al. 2016).

## Acknowledgements

This research was supported by Basic Science Research Program through the National Research Foundation of Korea funded by the Ministry of Education (NRF-2015R1D1A1A01056750) and Research Resettlement Fund for the new faculty of Seoul National University. We acknowledge the C.M. Rick Tomato Genetics Resource Center (University of California at Davis) for kindly providing tomato seed stocks. G.A.H. acknowledges support from the National Science Foundation (grants DBI-0604336 and IOS-1456864) and AgBioResearch at Michigan State University.

## Authors' Contributions

GAH and JHK prepared manuscript, and NRJ, HK, ITH, and JHK performed research. GAH, NRJ, and JHK participated in its design and coordination of research and helped to draft the manuscript.

## Supporting Information

**Fig. S1.** Predicted mRNA sequence (A) and amino acid sequence (B) of ARPC2A from WT plants.
**Fig. S2.** Genomic sequence of the affected region of *ARPC2A* in WT and *ini* plants.
**Table S1.** Description of PCR-based mapping markers.
**Table S2.** Description of primers for RT-PCR and genomic PCR.
**Table S3.** Description of flanking PCR primers.
**Table S4.** Description of PCR primers used for probe synthesis.

## References

Basu D, El-Assal SED, Le J, Mallery EL, Szymanski DB (2004) Interchangeable functions of Arabidopsis PIROGI and the human WAVE complex subunit SRA1 during leaf epidermal development. Development 131:4345–4355

Basu D, Le J, El-Essal SED, Huang S, Zhang CH, Mallery EL, Koliantz G, Staiger CJ, Szymanski DB (2005) DISTORTED3/SCAR2 is a putative Arabidopsis WAVE complex subunit that activates the Arp2/3 complex and is required for epidermal morphogenesis. Plant Cell 17:502–524

Bleeker PM, Mirabella R, Diergaarde PJ, VanDoorn A, Tissier A, Kant MR, Prins M, de Vos M, Haring MA, Schuurink RC (2012) Improved herbivore resistance in cultivated tomato with the sesquiterpene biosynthetic pathway from a wild relative. P Natl Acad Sci 109:20124–20129

Campbell BW, Hofstad AN, Sreekanta S, Fu F, Kono TJY, O'Rourke JA, Vance CP, Muehlbauer GJ, Stupar RM (2016) Fast neutron-induced structural rearrangements at a soybean *NAP1* locus result in *gnarled* trichomes. Theor Appl Genet 129:1725–1738

Chang J, Yu T, Gao SH, Xiong C, Xie QM, Li HX, Ye ZB, Yang CX (2016) Fine mapping of the *dialytic* gene that controls multicellular trichome formation and stamen development in tomato. Theor Appl Genet 129:1531–1539

Deeks MJ, Kaloriti D, Davies B, Malho R, Hussey PJ (2004) Arabidopsis NAP1 is essential for Arp2/3-dependent trichome morphogenesis. Curr Biol 14:1410–1414

Dempsey WH, Sherif THI (1987) Genetic and morphological comparisons of 7 “*hairless*” mutants in the tomato. Rep Tomato Genet Coop 37:43–44

Dyachok J, Zhu L, Liao FQ, He J, Huq E, Blancaflor EB (2011) SCAR mediates light-induced root elongation in Arabidopsis through photoreceptors and proteasomes. Plant Cell 23:3610–3626

Ehleringer JR, Mooney HA (1978) Leaf hairs: Effects on physiological

activity an adaptive value to a desert shrub. Oecologia 37:183–200
El-Assal SE, Le J, Basu D, Mallery EL, Szymanski DB (2004) DISTORTED2 encodes an ARPC2 subunit of the putative Arabidopsis ARP2/3 complex. Plant J 38:526–538
Eshed Y, Zamir D (1995) An introgression line population of *Lycopersicon pennellii* in the cultivated tomato enables the identification and fine mapping of yield-associated QTL. Genetics 141:1147–1162
Gan YB, Kumimoto R, Liu C, Ratcliffe O, Yu H, Broun P (2006) GLABROUS INFLORESCENCE STEMS modulates the regulation by gibberellins of epidermal differentiation and shoot maturation in Arabidopsis. Plant Cell 18:1383–1395
Gavrin A, Jansen V, Ivanov S, Bisseling T, Fedorova E (2015) ARP2/3-mediated actin nucleation associated with symbiosome membrane is essential for the development of symbiosomes in infected cells of *Medicago truncatula* root nodules. Mol Plant Microbe In 28:605–614
Goffreda JC, Steffens JC, Mutschler MA (1990) Association of epicuticular sugars with aphid resistance in hybrids with wild Tomato. J Am Soc Hortic Sci 115:161–165
Grebe M (2012) The patterning of epidermal hairs in Arabidopsis - updated. Curr Opin Plant Biol 15:31–37
Hossain MS, Liao JQ, James EK, Sato S, Tabata S, Jurkiewicz A, Madsen LH, Stougaard J, Ross L, Szczyglowski K (2012) *Lotus japonicus ARPC1* is required for rhizobial infection. Plant Physiol 160:917–928
Jiang K, Sorefan K, Deeks MJ, Bevan M, Hussey PJ, Hetherington AM (2012) The ARP2/3 Complex mediates guard cell actin reorganization and stomatal movement in Arabidopsis. Plant Cell 24:2031–2040
Juvik JA, Shapiro JA, Young TE, Mutschler MA (1994) Acylglucoses from wild tomatoes alter behavior and reduce growth and survival of *Helicoverpa zea* and *Spodoptera exigua* (Lepidoptera, Noctuidae). J Econ Entomol 87:482–492
Kang JH, Shi F, Jones AD, Marks MD, Howe GA (2010a) Distortion of trichome morphology by the *hairless* mutation of tomato affects leaf surface chemistry. J Exp Bot 61:1053–1064
Kang JH, Campos ML, Zemelis-Durfee S, Al-Haddad JM, Jones AD, Telewski FW, Brandizzi F, Howe GA (2016) Molecular cloning of the tomato *Hairless* gene implicates actin dynamics in trichome-mediated defense and mechanical properties of stem tissue. J Exp Bot 67:5313–5324
Kang JH, Liu GH, Shi F, Jones AD, Beaudry RM, Howe GA (2010b) The tomato *odorless-2* mutant is defective in trichome-based production of diverse specialized metabolites and broad-spectrum resistance to insect herbivores. Plant Physiol 154:262–272
Kang JH, McRoberts J, Shi F, Moreno JE, Jones AD, Howe GA (2014) The flavonoid biosynthetic enzyme chalcone isomerase modulates terpenoid production in glandular trichomes of tomato. Plant Physiol 164:1161–1174
Karabourniotis G, Papadopoulos K, Papamarkou M, Manetas Y (1992) Ultraviolet-B radiation absorbing capacity of leaf hairs. Physiologia Plantarum 86:414–418
Kennedy GG (2003) Tomato, pests, parasitoids, and predators: tritrophic interactions involving the genus *Lycopersicon*. Annu Rev Entomol 48:51–72
Le J, Mallery EL, Zhang CH, Brankle S, Szymanski DB (2006) Arabidopsis BRICK1/HSPC300 is an essential WAVE-complex subunit that selectively stabilizes the Arp2/3 activator SCAR2. Curr Biol 16:895–901
Lee DK, Park SH, Seong SY, Kim YS, Jung H, Do Choi Y, Kim JK (2016) Production of insect-resistant transgenic rice plants for use in practical agriculture. Plant Biotechnol Rep 10:391–401
Li LJ, Ren F, Gao XQ, Wei PC, Wang XC (2013) The reorganization of actin filaments is required for vacuolar fusion of guard cells during stomatal opening in Arabidopsis. Plant Cell Environ 36:484–497
Luckwill LC (1943) The *genus* Lycopersicon: *a historical, biological and taxonomic survey of the wild and cultivated tomatoes*. UK: University of Aberdeen
Miyahara A, Richens J, Starker C, Morieri G, Smith L, Long S, Downie JA, Oldroyd GED (2010) Conservation in function of a SCAR/WAVE component during infection thread and root hair growth in *Medicago truncatula*. Mol Plant Microbe In 23:1553–1562
Oppenheimer DG, Pollock MA, Vacik J, Szymanski DB, Ericson B, Feldmann K, Marks MD (1997) Essential role of a kinesin-like protein in Arabidopsis trichome morphogenesis. P Natl Acad Sci 94:6261–6266
Payne T, Clement J, Arnold D, Lloyd A (1999) Heterologous myb genes distinct from *GL1* enhance trichome production when overexpressed in *Nicotiana tabacum*. Development 126:671–682
Qian P, Hou S, Guo G (2009) Molecular mechanisms controlling pavement cell shape in Arabidopsis leaves. Plant Cell Rep 28:1147–1157
Qiu LP, Lin JS, Xu J, Sato S, Parniske M, Wang TL, Downie JA, Xie F (2015) SCARN a novel class of SCAR protein that is required for root-hair infection during legume nodulation. PLoS Genet 11
Ramsay NA, Glover BJ (2005) MYB-bHLH-WD40 protein complex and the evolution of cellular diversity. Trends Plant Sci 10:63–70
Reeves AF (1977) Tomato trichomes and mutations affecting their development. Am J Bot 64:186–189
Robinson RC, Turbedsky K, Kaiser DA, Marchand JB, Higgs HN, Choe S, Pollard TD (2001) Crystal structure of Arp2/3 complex. Science 294:1679–1684
Rodriguez AE, Tingey WM, Mutschler MA (1993) Acylsugars of *Lycopersicon pennellii* deter settling and feeding of the green peach Aphid (Homoptera, Aphididae). J Econ Entomol 86:34–39
Sallaud C, Rontein D, Onillon S, Jabes F, Duffe P, Giacalone C, Thoraval S, Escoffier C, Herbette G, Leonhardt N, Causse M, Tissier A (2009) A novel pathway for sesquiterpene biosynthesis from Z,Z-Farnesyl Pyrophosphate in the wild tomato *Solanum habrochaites*. Plant Cell 21:301–317
Schilmiller AL, Charbonneau AL, Last RL (2012) Identification of a BAHD acetyltransferase that produces protective acyl sugars in tomato trichomes. P Natl Acad Sci 109:16377–16382
Schilmiller AL, Schauvinhold I, Larson M, Xu R, Charbonneau AL, Schmidt A, Wilkerson C, Last RL, Pichersky E (2009) Monoterpenes in the glandular trichomes of tomato are synthesized from a neryl diphosphate precursor rather than geranyl diphosphate. P Natl Acad Sci 106:10865–10870
Serna L, Martin C (2006) Trichomes: different regulatory networks lead to convergent structures. Trends Plant Sci 11:274–280
Shepherd RW, Bass WT, Houtz RL, Wagner GJ (2005) Phylloplanins of tobacco are defensive proteins deployed on aerial surfaces by short glandular trichomes. Plant Cell 17:1851–1861
Stubbe H (1964) Mutanten der kulturtomate *Lycopersicon esculentum* Miller VI. kulturpflanze 12:121–152
Szymanski DB (2005) Breaking the WAVE complex: the point of Arabidopsis trichomes. Curr Opin Plant Biol 8:103–112
Szymanski DB, Jilk RA, Pollock SM, Marks MD (1998) Control of *GL2* expression in Arabidopsis leaves and trichomes. Development 125:1161–1171
Tanksley SD, Ganal MW, Prince JP, Devicente MC, Bonierbale MW, Broun P, Fulton TM, Giovannoni JJ, Grandillo S, Martin GB, Messeguer R, Miller JC, Miller L, Paterson AH, Pineda O, Roder MS, Wing RA, Wu W, Young ND (1992) High density molecular linkage maps of the tomato and potato genomes.

Genetics 132:1141–1160
Thole V, Alves SC, Worland B, Bevan MW, Vain P (2009) A protocol for efficiently retrieving and characterizing flanking sequence tags (FSTs) in *Brachypodium distachyon* T-DNA insertional mutants. Nat Protoc 4:650–661
Tomato Genome Consortium (2012) The tomato genome sequence provides insights into fleshy fruit evolution. Nature 485:635–641
Uhrig JF, Mutondo M, Zimmermann I, Deeks MJ, Machesky LM, Thomas P, Uhrig S, Rambke C, Hussey PJ, Huelskamp M (2007) The role of Arabidopsis SCAR genes in ARP2-ARP3-dependent cell morphogenesis. Development 134:967–977
Walker JD, Oppenheimer DG, Concienne J, Larkin JC (2000) *SIAMESE*, a gene controlling the endoreduplication cell cycle in *Arabidopsis thaliana* trichomes. Development 127:3931–3940
Wang PW, Richardson C, Hawes C, Hussey PJ (2016) Arabidopsis NAP1 regulates the formation of autophagosomes. Curr Biol 26:2060–2069
Williams WG, Kennedy GG, Yamamoto RT, Thacker JD, Bordner J (1980) 2-Tridecanone: A naturally occurring insecticide from the wild tomato *Lycopersicon hirsutum f.Glabratum*. Science 207:888–889
Yan A, Wu MJ, Zhao YQ, Zhang AD, Liu BH, Schiefelbein J, Gan YB (2014) Involvement of C2H2 zinc finger proteins in the regulation of epidermal cell fate determination in Arabidopsis. J Integr Plant Biol 56:1112–1117
Yang C, Li H, Zhang J, Luo Z, Gong P, Zhang C, Li J, Wang T, Zhang Y, Lu Ye, Ye Z (2011) A regulatory gene induces trichome formation and embryo lethality in tomato. P Natl Acad Sci 108:11836–11841
Yang C, Ye Z (2013) Trichomes as models for studying plant cell differentiation. Cell Mol Life Sci 70:1937–1948
Zhao M, Morohashi K, Hatlestad G, Grotewold E, Lloyd A (2008) The TTG1-bHLH-MYB complex controls trichome cell fate and patterning through direct targeting of regulatory loci. Development 135:1991–1999
Zhao Y, Pan Z, Zhang Y, Qu XL, Zhang YG, Yang YQ, Jiang XN, Huang SJ, Yuan M, Schumaker KS, Guo Y (2013) The Actin-related protein2/3 Complex regulates mitochondrial-associated calcium signaling during salt stress in Arabidopsis. Plant Cell 25:4544–4559
Zhou WQ, Wang YC, Wu ZL, Luo L, Liu P, Yan LF, Hou SW (2016) Homologs of SCAR/WAVE complex components are required for epidermal cell morphogenesis in rice. J Exp Bot 67:4311–4323
Zobel RW, Opena RT, Rick CM (1970) Additional linkages of the stubbe series. Rep Tomato Gen Coop 20:69–71